

Utilizing Imogolite Nanotubes as a Tunable Catalytic Material for the Selective Isomerization of
Glucose to Fructose

Undergraduate Research Thesis

Presented in Partial Fulfillment of the Requirements for Graduation with Honors Research
Distinction in the College of Engineering of The Ohio State University

By Nathaniel Olson

William G. Lowrie Department of Chemical and Biomolecular Engineering

The Ohio State University

2018

Thesis Committee:

Dr. Nicholas Brunelli, Adviser

Dr. Stuart Cooper

© Copyright by

Nathaniel Olson

2018

Abstract

The isomerization of glucose to fructose is an important step in the conversion of biomass to valuable fuels and chemicals. A key challenge for the isomerization reaction is achieving high selectivity towards fructose using recyclable and inexpensive catalysts. Imogolite is a single-walled aluminosilicate nanotube characterized by surface areas of 200-400 m²/g and pore widths near 1 nm. In this study, imogolite nanotubes are used as a heterogeneous catalyst for the isomerization of glucose to fructose. Catalytic testing demonstrates the catalytic activity of imogolite for the isomerization of glucose to fructose. Imogolite is a highly tunable structure and can be modified through substitution of Si with Ge or through functionalization of methyl groups to the inner surface. These modifications change the surface properties of the nanotubes and enable tuning of the catalytic performance. Aluminosilicate imogolite is the most active material for the conversion of glucose. Conversion of glucose of 30% and selectivity for fructose of 45% is achieved using aluminosilicate imogolite. Modification of imogolite with germanium or methyl groups decreases the conversion, but increases the selectivity. Generally, the selectivity for fructose decreases as the conversion of glucose increases. Interestingly, the imogolite nanotubes have comparable catalytic selectivity at similar conversion as base catalyzed reactions. Catalyst recycling experiments revealed that organic content accumulates on the nanotubes that results in a minor reduction in conversion while maintaining similar catalytic selectivity. Overall, imogolite nanotubes demonstrate an active and tunable catalytic platform for the isomerization of glucose to fructose.

Acknowledgments

First and foremost, I want to thank Dr. Nicholas Brunelli for his guidance and mentorship. Not only on this project, but on life, learning, and research. This work would not have been possible without Dr. Brunelli's support. I would also like to thank all members of the Catalytic Design Group for their help and support, especially Nitish Deshpande. Nitish, thank for teaching me the fine art of catalytic testing. Also, thank you for all the catalytic tests you ran yourself, especially those at the very beginning which served as the impetus for the project.

Vita

2018.....B.S. Chemical Engineering, The Ohio State University, Columbus, OH

2017.....Materials Research Intern, NASA Glenn Research Center, Cleveland, OH

2014.....Tinora High School, Defiance, OH

Fields of Study

Major Field: Chemical Engineering

Table of Contents

Abstract	ii
Acknowledgments.....	iii
Vita.....	iv
List of Tables	vi
List of Figures	vii
Chapter 1. Introduction	1
Chapter 2. Materials and Methods.....	5
2.1. Imogolite Synthesis.....	5
2.2 Material Characterization.....	6
2.3 Catalytic Testing	7
2.4 Catalyst Reuse Testing.....	7
Chapter 3. Results and Discussion.....	8
3.1. Catalyst Synthesis and Characterization.....	8
3.2. XRD Results	8
3.3. N ₂ Physisorption Results.....	10
3.4. Glucose to Fructose Isomerization Results.....	11
3.5. Catalyst Reuse Testing.....	18
Chapter 4. Conclusions	20
Bibliography	21
Appendix A. Supplementary Information.....	25

List of Tables

Table 1: Nitrogen physisorption results for imogolite. Pore width increases as substitution of Si increases, with a more dramatic effect in Me-IMO. Surface areas are highest for Me-IMO materials.	11
---	----

List of Figures

- Figure 1:** The cross-section of an imogolite nanotube. The nanotube is composed of an rolled gibbsite sheet with an inner wall of silanol (Si-OH) groups.¹⁷ 3
- Figure 2:** Powder x-ray diffraction pattern of AlSi imogolite compared to Ge-IMO of 30 and 80%. The AlSi IMO is in black with Ge-0.3-IMO in blue and Ge-0.80-IMO in orange. 9
- Figure 3:** Powder x-ray diffraction pattern of AlSi imogolite compared to Me-IMO of 50 and 100%. The AlSi IMO is in black with Me-0.5-IMO in teal and Me-1.0-IMO in pink. 9
- Figure 4:** Kinetic evaluation of IMO-R over 48 hours. Data points were collected at 2, 6, 16, 20, 24, and 48 hours. The test was performed using 100 mg of IMO at 100 °C with 1 g of 10 wt% glucose solution. The glucose conversion is in red (left axis) and fructose selectivity is in blue (right axis)..... 12
- Figure 5:** The effect of temperature on the conversion and selectivity of imogolite compared to other catalysts. Selectivity is on the y-axis and conversion is on the x-axis. For the IMO catalysts, blue is 100 °C and red is 120 °C. Other catalysts included are KOH, NaX Zeolite, Sn β zeolite, TEA, Immobilized TEA.^{28,29,12,4,9,10} 14
- Figure 6:** Activity of the imogolite catalysts at 100°C for 24 hr. All tests were performed with 100 mg of catalyst and 1 g of 10 wt% glucose solution. Both conversion and selectivity are on the y-axis with conversion in red and selectivity in blue..... 16
- Figure 7:** Activity of the imogolite catalysts at 120°C for 24 hr. All tests were performed with 100 mg of catalyst and 1 g of 10 wt% glucose solution. Both conversion and selectivity are on the y-axis with conversion in red and selectivity in blue..... 16
- Figure 8:** TGA mass loss curve of as-synthesized IMO and recycled IMO after three reactions. The as-synthesized IMO is in black and the recycled IMO is in green. 19

Chapter 1. Introduction

Creating sustainable methods to produce chemicals and fuels can be achieved through identifying robust and stable catalytic materials for conversion of biomass. Indeed, the primary challenges for biomass conversion is achieving high selectivity with a stable heterogeneous catalytic material. One important chemical reaction for biomass conversion is the isomerization of glucose to fructose.¹ This reaction remains an important bottleneck in producing the important intermediate 5-hydroxymethylfurfuraldehyde (HMF), which is considered the most important chemical to produce to enable large scale biomass processing.² The importance of this overall reaction sequence merits investigation of alternative catalytic materials.

Several intriguing catalysts for this reaction have been investigated, including enzymes, Lewis acids, inorganic Brønsted bases, and organic bases.³⁻¹⁰ The most common industrial catalyst for isomerization of glucose to fructose is the enzyme glucose isomerase. Though enzymes are widely used for food applications, it is necessary to maintain strict control of pH, temperature, and feed purity to avoid catalyst deactivation.³ With the hopes of expanding glucose isomerization to enable large scale biomass conversion, the need to develop more robust catalytic materials inspired investigation of the Lewis acidic catalyst Sn-BEA that has been shown to selectively convert glucose to fructose.⁴ This work has sparked interest in catalysts for the isomerization of glucose to fructose though commercial utilization would require improving catalyst lifetime since Sn-BEA undergoes deactivation via leaching of Sn active sites.¹¹ Several inorganic base catalysts have been identified for the reaction including $\text{Ca}(\text{OH})_2$ and NaOH .⁵⁻⁶ The yield of fructose achieved with these catalysts are low because of the instability of monosaccharides when exposed to base

catalysts. Furthermore, these catalysts are homogeneous and cannot be recycled. Intriguing work has also investigated organic base such as triethylamine.^{9,10} Homogeneous triethylamine exhibited good catalytic activity and selectivity, inducing researchers to investigate heterogeneous catalysts such as poly(ethylene imine) (PEI) and tertiary amines immobilized on silica materials.^{9,10} These catalysts tended to deactivate via leaching and formation of an acidic byproduct that is currently unknown, though the catalysts could be regenerated. Combining the ideas of using zeolites and base catalyst, researchers have investigated sodium-exchanged zeolites.¹² These catalysts are active and selective, but deactivate via leaching of the basic sodium species, making constant regeneration of the active site necessary. The concept of base catalyzed glucose isomerization certainly has merit, provided that the deactivation could be limited.

An interesting alternative catalytic material that has received limited investigation is imogolite. Imogolite is a naturally occurring aluminosilicate nanotube with an empirical formula of $(\text{OH})_3\text{Al}_2\text{O}_3\text{SiOH}$ that was first discovered in 1962 in volcanic-ash derived soils in Japan.¹³ A synthetic procedure was first described in 1977 based upon the conditions in which imogolite formed.¹⁴ This procedure has been optimized over the years, and it can be synthesized with monodisperse and tunable dimensions and composition.¹⁵⁻¹⁷ A cross-section of an imogolite nanotube is seen in Figure 1. Imogolite nanotubes have a diameter of 2 nm and range in length from 100 to 1000 nm. Currently, limited characterization has been performed to determine the nature of the surface properties of the catalytic materials.

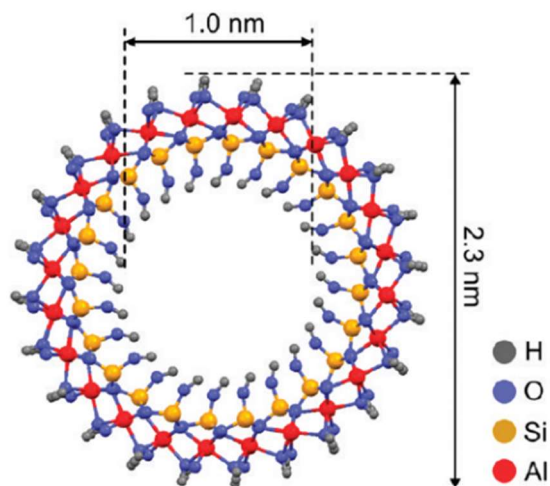


Figure 1: The cross-section of an imogolite nanotube. The nanotube is composed of an rolled gibbsite sheet with an inner wall of silanol (Si-OH) groups.¹⁷

Several modifications have been performed on imogolite that could provide the ability to control its properties on the nanoscale. Aluminogermanate imogolite has been synthesized with up to 100% substitution of silicon with germanium. The resulting nanotubes have larger, tunable diameters and can form double-walled nanotubes.^{16,18,19} Interior surface modification with organic groups has also been performed using acetyl chloride, methyltrimethoxysilane, and trichlorosilane.¹⁷ The organic groups adjust the composition, hydrophobicity, and dimensions of the nanotube. Iron-doped imogolite has been synthesized as a potential catalyst for oxidation reactions.²⁰ Gold nanoparticle and imogolite composites have been fabricated for use as a catalyst or a coloring agent.²¹ Additionally, silver nanoparticles were immobilized on imogolite and showed antibacterial properties.²² It has also been shown that the phosphate groups of DNA interact with the aluminol groups on imogolite, which was utilized to form imogolite/DNA hybrid hydrogels.²³ These experiments demonstrate that imogolite is a tunable platform.

The high level of modification offered by imogolite presents tunable catalytic platform. Yet, little work has been done on application of imogolite nanotubes, especially in the realm of catalysis.^{24,25} To evaluate the promise that imogolite holds as tunable heterogeneous catalytic platform, it is important to elucidate structure-function relationships of the modifications that have been performed. Identification of design elements of imogolite would offer the ability to tune its properties and enable its use as an effective catalytic platform.

In this work, imogolite is investigated as a catalyst for the selective isomerization of glucose to fructose. The work examines the effect of modifying the composition of the imogolite nanotubes through including germanium and methyl substitution to alter the surface properties and catalytic performance. The most selective material is subjected to recycle experiments to determine the robustness of the catalytic material. Overall, this work provides insight on the catalytic activity in imogolite and its promise as a tunable, heterogeneous catalytic platform.

Chapter 2. Materials and Methods

2.1. Imogolite Synthesis

Perchloric acid is diluted to 38 mM from a 70wt% (11.595 M) stock solution. To do this, 5.454 g of 70wt% perchloric acid is diluted to 1000 mL with DI water. Precursors to imogolite are mixed in a glove box filled with nitrogen. For aluminosilicate imogolite (Al-Si IMO), aluminum-tri-sec-butoxide (4.680 g) is mixed with tetraethylorthosilicate (1.979 g) in a glass vial and shaken vigorously. This precursor mixture is then added to a 38 mM HClO₄ solution (250 mL) in a 2 L round-bottom flask under stirring at room temperature. The final molar ratio is Si:Al:HClO₄ of 1:2:1. The solutions are stirred at room temperature for 24 h. The solution is then diluted by a factor of 3.8 with DI water (700 mL) and stirred at 95°C for 4 days. After this period, the solution is allowed to cool to room temperature and concentrated using one of two methods. The first method involves concentrating the reaction mixture by a factor of 10 to approximately 100 mL using a rotary evaporator. Materials concentrated using a rotary evaporator are labeled with “R”. All materials modified with germanium and methyl functionalization are concentrated using the rotovap method. For the second method of concentration, a 30wt% ammonia solution is added dropwise until gelation occurs and a pH of 10 is reached. The gels are then centrifuged at 9000 rpm for 10 min and the supernatant is discarded. The nanotubes are dispersed by adding a few drops of hydrochloric acid to the gel with fuming observed. Materials concentrated using this acid-base addition method are labeled with “AB”. The gels obtained by both methods are added to a 15,000 kDa membrane submerged in DI water. The water is exchanged daily for 5 days. The

purified gels are dried at 80°C and the resulting solids are ground vigorously to obtain imogolite nanotubes as a fine powder.

For germanium imogolite (Ge-x-IMO), aluminum-tri-sec-butoxide is mixed with germanium(IV) ethoxide and tetraethylorthosilicate in a molar ratio of Si:Ge:Al:HClO₄ of 1-x:x:2:1. For Ge-0.3-IMO, this corresponds to 4.680 g aluminum-tri-sec-butoxide, 0.721 g germanium(IV) ethoxide, and 1.385 g TEOS. For Ge-0.8-IMO, 4.680 g aluminum-tri-sec-butoxide, 1.922 g germanium(IV) ethoxide, and 0.396 g TEOS.

For methyl imogolite (Me-x-IMO), aluminum-tri-sec-butoxide is mixed with methyltrimethoxysilane (Me-Si) and tetraethylorthosilicate in a molar ratio of Si:Me-Si:Al:HClO₄ of 1-x:x:2:1. For Me-0.5-IMO, this corresponds to 4.680 g aluminum-tri-sec-butoxide, 0.647 g methyltrimethoxysilane, and 0.990 g TEOS. For Me-1.0-IMO, 4.680 g aluminum-tri-sec-butoxide and 1.294 g methyltrimethoxysilane.

2.2 Material Characterization

The materials are characterized using standard techniques, including nitrogen physisorption, x-ray diffraction (XRD), and thermogravimetric analysis with differential scanning calorimetry (TGA-DSC). The textural properties are analyzed using a Micromeritics 3Flex surface characterization analyzer. The surface area is calculated using the BET method and the pore size is calculated using the HK method. Powder x-ray diffraction data are collected on a Bruker D8 Advance powder diffractometer (40 kV, 40 mA, sealed Cu X-ray tube) equipped with a Lynxeye XE-T position sensitive detector in Bragg-Brentano geometry. TGA-DSC are performed using STA 449 F5 Jupiter® (NETZSCH Instruments). The analysis is performed under flowing air (20

mL/min) and nitrogen (20 mL/min) at a ramp rate of 10°C/min from 30°C to 900°C followed by a 5 min hold at 900°C.

2.3 Catalytic Testing

A bulk solution containing 4.0 g dextrose and 36.0 g DI water is prepared. Two grams of the bulk solution is combined with 100 mg of catalyst in a 15 mL pressure tube. The tubes are submersed in a silicone oil bath at 100 °C at 420 rpm. After 24 hours, the tubes are transferred to an ice bath for 15 min. The solution is diluted with 2 g of 0.3 M d-mannitol solution (internal standard for HPLC measurements) and 30 g of DI water. The solution is centrifuged at 9000 rpm for 15 min and the supernatant is filtered using a 0.22 µm nylon (Ø = 13 mm) syringe filter and analyzed using High Performance Liquid Chromatography (HPLC) from Waters (Acquity) equipped with a refractive index (RI) detector. Glucose, fructose, and mannitol concentrations were monitored using Waters Sugar Pak-1 column equipped with a pre-column filter. DI water was used as the mobile phase at a flow rate of 0.20 mL/min and a column temperature of 70 °C.

2.4 Catalyst Reuse Testing

Catalyst reuse testing was also performed. The reaction began with 300 mg of catalyst and 3.0 g of 10wt% glucose solution. Following the reaction, the solution was diluted and centrifuged as described previously. The supernatant was completely removed to separate the catalyst. The catalyst was washed three times with DI water and centrifuged after each wash. The catalyst was dried overnight at 80 °C. The mass of the catalyst was obtained and then added to an amount of 10wt% glucose solution that corresponds to 100 mg catalyst per 1 g of 10wt% glucose solution.

Chapter 3. Results and Discussion

3.1. Catalyst Synthesis and Characterization

Imogolite nanotubes are successfully synthesized utilizing the procedure described previously. For all variations of imogolite, the solution turns cloudy upon combination of precursors and the HClO_4 solution. For the Al-Si and Ge-IMO, the solution then turns clear approximately 1 hour after heating to 95 °C. The Me-IMO remains cloudy throughout the synthesis, likely because of the increased hydrophobicity of the material.¹⁷ Concentration via the rotovap method yields a cloudy solution. The acid-base method yields a gel-like solution. After drying, both result in a sheet-like material that must be ground vigorously to yield imogolite as a fine powder.

3.2. XRD Results

The XRD pattern of Al-Si IMO its peaks are used to compare against Ge- and Me-IMO in Figures 2 and 3, respectively. The important characteristic peaks of imogolite occur near 4, 9, 13, 28, and 40° 2 θ . The characteristic peaks of imogolite remain in the Ge-IMO samples, though other peaks begin to form near 10° at 30% Ge and increase in intensity at 80% Ge. This change in diffraction pattern is typical of the formation of Ge-IMO. The shift of the first peak indicates a change in the inner diameter of the nanotube. Specifically, a shift to the left is indicative of a larger inner diameter. The Me-IMO patterns in Figure 3 contain the characteristic peaks of imogolite. With increasing methyl content, a sharp feature forms near 20° that indicates long-range order or crystallinity. The presence of the characteristic peaks are consistent with the formation of imogolite nanotubes. We hypothesize the sharp peaks indicate the formation of a crystalline phase

or the presence of long-range order among the imogolite nanotubes. It can be seen in the peaks at 4 and 9° that sharpness and intensity increase, further evidence of increased crystallinity.

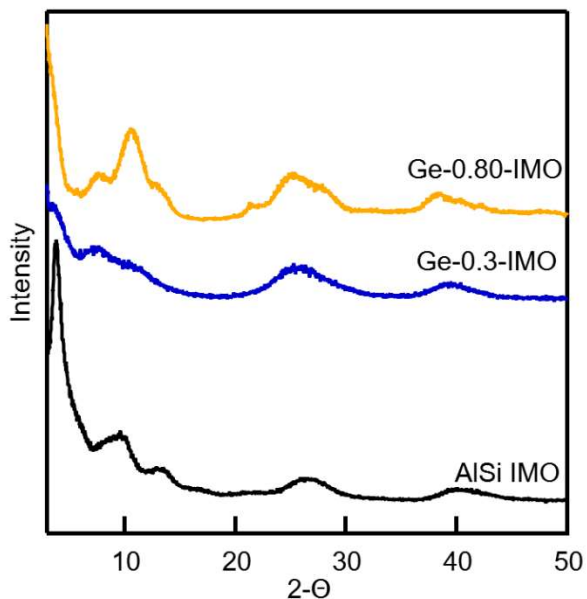


Figure 2: Powder x-ray diffraction pattern of AlSi imogolite compared to Ge-IMO of 30 and 80%. The AlSi IMO is in black with Ge-0.3-IMO in blue and Ge-0.80-IMO in orange.

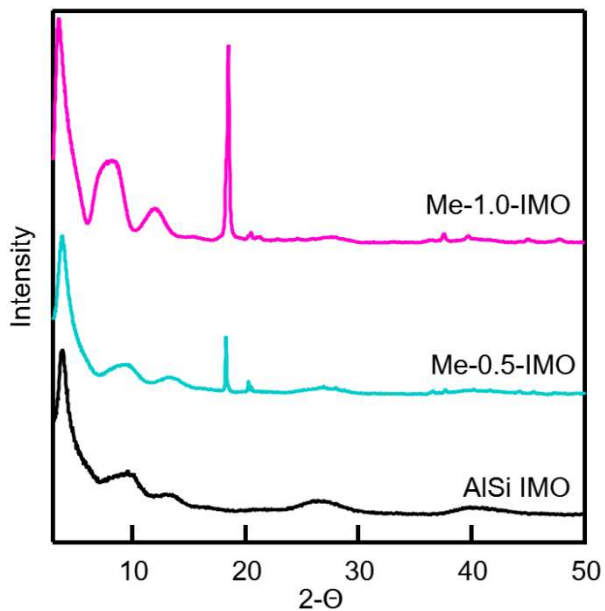


Figure 3: Powder x-ray diffraction pattern of AlSi imogolite compared to Me-IMO of 50 and 100%. The AlSi IMO is in black with Me-0.5-IMO in teal and Me-1.0-IMO in pink.

3.3. *N₂ Physisorption Results*

The effects of composition on surface area and pore properties of imogolite are analyzed with nitrogen physisorption. Table 1 provides a summary of imogolite materials analyzed with nitrogen physisorption. A single sample of AlSi imogolite is split into two to analyze the effect of concentration method on the surface properties of imogolite. For the rotovap method, the sample has a surface area of 273 m²/g with a pore width of 0.88 nm. For the acid-base method, the surface area is 288 m²/g with a pore width of 0.88 nm. These results demonstrate that the method of concentration does not have a significant impact on the surface properties of imogolite.

Germanium substitution results in changes to the surface area and pore width. Increasing the germanium content leads to slightly higher surface areas. Introduction of Ge into IMO also results in an increased pore width according to nitrogen physisorption, which is corroborated by the shift to the left in the first peak of the XRD patterns. At 30% Ge, a pore width of 0.91 nm is achieved, which is greater than the pure IMO. The pore width then further increases to 0.95 nm for 80% Ge. The increase in pore width can be explained by the increase in bond length from Si-O to Ge-O, as has been previously reported.²⁶

Methyl substitution leads to an increase in pore size, from 0.94 nm at 50% methyl to 1.10 nm at 100% methyl. The presence of methyl groups on the inner surface of the nanotube may increase the pore size. The surface areas for these materials are generally higher than Al-Si IMO, 456 and 366 m²/g at 50% and 100% methyl, respectively. It is hypothesized this increase occurs on account of the increased hydrophobicity of the material. Though all materials undergo heating

under vacuum to remove any adsorbed compounds, it is possible water remains strongly adsorbed to pure imogolite.¹⁷ It has been shown previously that the degas temperature has a strong effect on measured surface area.²⁷ Introduction of methyl groups increase hydrophobicity and provide more available surface area for nitrogen physisorption.

Table 1: Nitrogen physisorption results for imogolite. The BET surface areas and HK pore widths of the AlSi IMO are compared to the Me and Ge modified materials.

Material	BET Surface Area (m ² /g)	HK Pore Width (nm)
IMO-R	273	0.88
IMO-AB	288	0.88
Me-0.5-IMO	456	0.94
Me-1.0-IMO	366	1.10
Ge-0.3-IMO	229	0.91
Ge-0.8-IMO	253	0.95

3.4. Glucose to Fructose Isomerization Results

Catalytic testing began with kinetic evaluation of AlSi imogolite concentrated using the rotovap method. Figure 2 depicts the change in conversion and selectivity over 48 hours for IMO-R. Conversion steadily increases with time and selectivity decreases with time. Although the isomerization of glucose to fructose is an equilibrium-limited reaction, equilibrium is not achieved using an imogolite catalyst. This test demonstrates the activity of imogolite for the isomerization of glucose. After 48 hours, the imogolite catalyst has converted 35% of the glucose with 40%

selectivity for fructose. Conversion continues to increase at 48 hours, evidence the sites are not poisoned and the catalyst does not undergo deactivation.

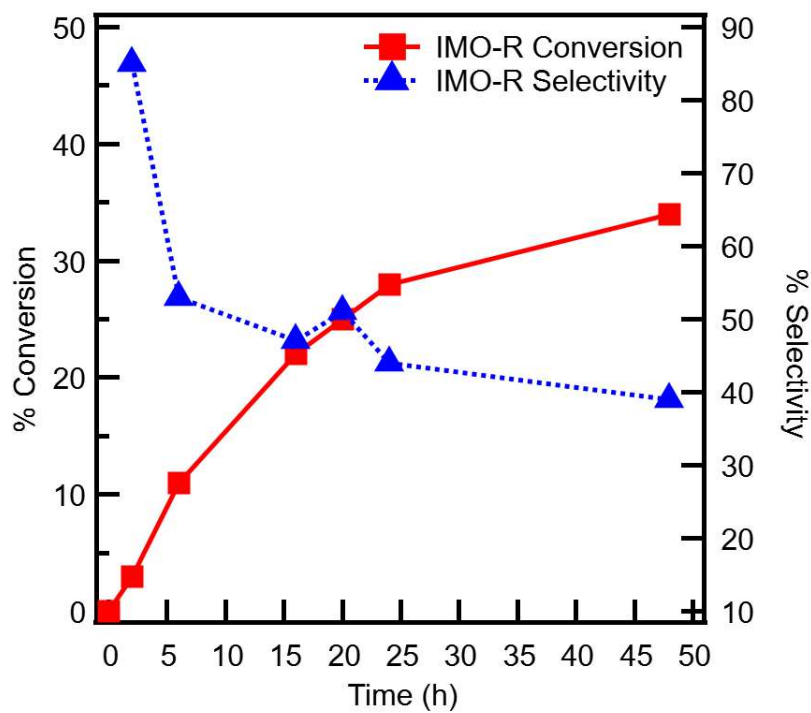


Figure 2: Kinetic evaluation of IMO-R over 48 hours. Data points were collected at 2, 6, 16, 20, 24, and 48 hours. The test was performed using 100 mg of IMO at 100 °C with 1 g of 10 wt% glucose solution. The glucose conversion is in red (left axis) and fructose selectivity is in blue (right axis).

The effect of concentration method for AlSi imogolite on catalytic activity is studied. At 100°C, there is no difference in the conversion and selectivity of imogolite concentrated using the rotovap and acid-base methods. The reaction is also run under inert nitrogen conditions. Relative to air, running the reaction under inert conditions decreases the observed conversion from 30% to 18% and selectivity increases from 45% to 57%. This result of increased selectivity with decreased conversion is consistent with other experiments to be discussed. The effect of increased selectivity under nitrogen is not observed, as has been previously reported.¹⁰ To investigate other routes of

increasing conversion of glucose, AlSi IMO is tested at an elevated temperature of 120 °C. The conversion increases from 30% to 74% when the temperature is increased. The 74% conversion is the highest achieved in this study. Meanwhile, the selectivity drops from 45% to 22%. Therefore, temperature provides an additional element of control over the catalytic activity of the material.

After demonstration of the catalytic activity of imogolite, the temperature of the reaction is studied. The temperature is found to have a significant effect on the conversion and selectivity of the reaction. When the reaction is run at 120 °C, the conversion increases significantly, but the selectivity decreases by nearly half. The highest selectivities for fructose are achieved at 100 °C. The increased conversion of glucose at a higher temperature is not surprising as dictated by kinetics. More interesting is that the dehydration of fructose to HMF occurs at elevated temperatures. Running the reaction with the imogolite catalyst leads to a 5-8% yield of HMF. This yield of HMF indicates the selectivity and yield of fructose are higher than reported for the imogolite catalyst, as some fructose is being dehydrated to HMF. Imogolite may also have the capability of serving as a catalyst for the dehydration of fructose into HMF. Figure 3 compares the selectivities and conversions achieved at the two reaction temperatures with alternative catalysts. All catalysts display a trend of decreasing selectivity for fructose with increasing conversion. Me-1.0-IMO deviates from this trend, as will be discussed further.

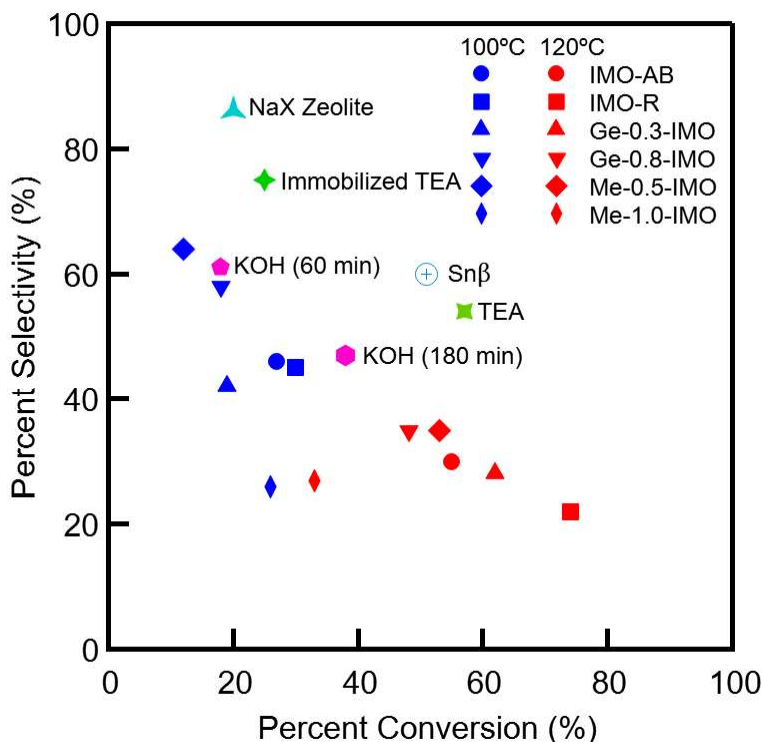


Figure 3: The effect of temperature on the conversion and selectivity of imogolite compared to other catalysts. Selectivity is on the y-axis and conversion is on the x-axis. For the IMO catalysts, blue is 100 °C and red is 120 °C. Other catalysts included are KOH, NaX Zeolite, Snβ zeolite, TEA, Immobilized TEA.^{28,29,12,4,9,10}

Modification of imogolite with germanium and methyl has an influence on the catalytic activity. Figure 4 and Figure 5 summarize the effect of modification at 100 and 120 °C, respectively. Introduction of 30% germanium in Ge-0.3-IMO decreases the conversion slightly and maintains a similar selectivity. For Ge-0.80-IMO, the conversion is further decreased and the selectivity is increased to 58%, compared to 45% for AlSi IMO. The decreased conversion and increased selectivity fits well with the linear trend established in Figure 5. As additional fructose is formed, degradation to other byproducts occurs. Furthermore, the effects of germanium substitution demonstrate the tunable nature of imogolite. Not only is imogolite an active catalyst,

but the activity can be tuned through simple changes to the structure and composition of the nanotube.

Functionalization of imogolite with methyl groups also has an effect on the catalytic activity. At low temperatures, the conversion of glucose is greatly depressed to 12% for Me-0.5-IMO. Meanwhile, the selectivity increases to 64%, the highest selectivity achieved in this study for any material. This data point again falls along the linear trend discussed previously, where selectivity increases as conversion decreases. At high temperatures, the effect of 50% methyl substitution is not as strong, though still present. Me-1.0-IMO deviates from the trend established in Figure 5. At 100 °C, Me-1.0-IMO has similar conversion to AlSi imogolite, but at much lower selectivity for fructose. Increasing the temperature only slightly increases the conversion and maintains a similar selectivity. This behavior is unique to all the imogolite materials studied. At 100% methyl loading, all the silanols are theoretically replaced with methyl groups. For this material, the selectivity is greatly diminished for Me-1.0-IMO compared to pure AlSi imogolite.

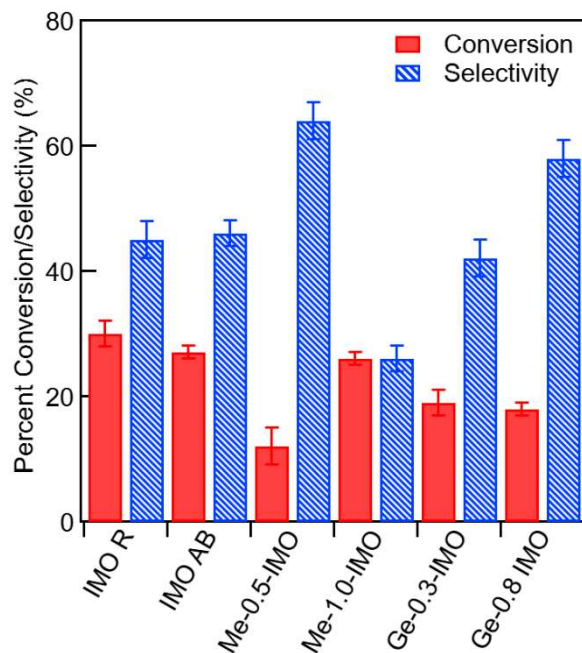


Figure 4: Activity of the imogolite catalysts at 100°C for 24 hr. All tests were performed with 100 mg of catalyst and 1 g of 10 wt% glucose solution. Both conversion and selectivity are on the y-axis with conversion in red and selectivity in blue.

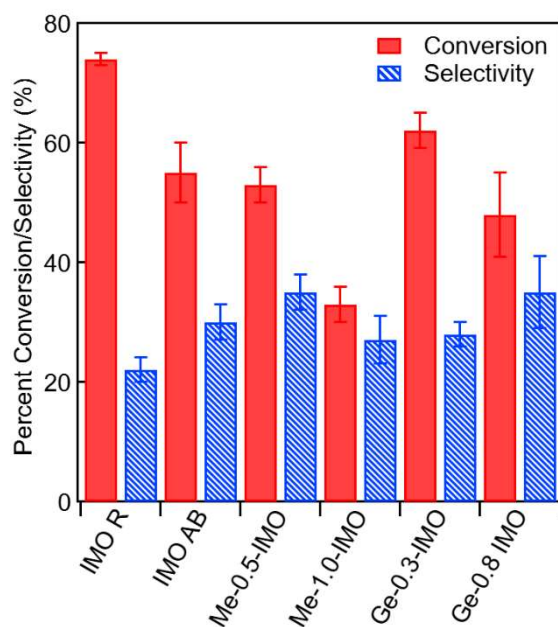


Figure 5: Activity of the imogolite catalysts at 120°C for 24 hr. All tests were performed with 100 mg of catalyst and 1 g of 10 wt% glucose solution. Both conversion and selectivity are on the y-axis with conversion in red and selectivity in blue.

The modification of imogolite has an effect on the structure and catalytic activity of the material. Highest conversions are achieved with AlSi IMO. Both modifications (Ge and Me) result in decreased conversion of glucose with higher selectivities for fructose. Increasing the temperature of the reaction further increases conversion of glucose but decreases the selectivity of the catalysts. While glucose conversion is desirable, high conversions result in low selectivity for fructose, the desired product. Selectivity is the key factor that must be optimized for the production of fructose as unreacted glucose can be utilized through recycle. The ability to control the structure and composition of imogolite, which has an effect on the catalytic activity, provides a new, tunable catalytic platform for the isomerization of glucose to fructose.

It is hypothesized the aluminol groups on the outer wall of the nanotube play a key role in the catalytic activity of imogolite. With 100% methyl content, the material still demonstrates catalytic activity. This provides evidence that silanol groups are not necessary for imogolite to convert glucose into fructose. The outer wall of imogolite is compared to a gibbsite $[\text{Al}(\text{OH})_3]$ sheet.^{27,30} Gibbsite, which is a mineral form of aluminum hydroxide, displays amphoteric behavior.³¹ In acidic conditions, gibbsite behaves as a Brønsted base and in basic conditions, as a Lewis acid. As mentioned previously, both Brønsted basic and Lewis acidic catalysts are active for the isomerization of glucose to fructose. The accessible surface area on the outer wall of the nanotube, comprised of a gibbsite sheet, provides the most likely source of the catalytic activity for imogolite.

Further investigation of imogolite and its active sites may lend to its use as an effective heterogeneous catalyst for other important reactions. Here, it is demonstrated that imogolite nanotubes are an effective catalyst for the isomerization of glucose to fructose. Formation of HMF

is a promising indication of its use as a catalyst for the dehydration of fructose to HMF. With the yields of fructose obtained in this study, the 5 to 8% yield of HMF is significant and warrants further study.

3.5. Catalyst Reuse Testing

Aluminosilicate imogolite underwent reuse tests, which involves scaling up the initial amount of catalyst to ensure recovery of sufficient material for subsequent tests. The recycle tests are performed at 100 °C for 24 hr. Initial conversion was 25% with a selectivity of 56%. The catalyst underwent deactivation, with conversion decreasing to 21% and 17% in the second and third tests. The selectivity decreased from 56% to 49% and remained at 49% for the third test. Following the three reactions, characterization is performed to provide insight on the mechanism of deactivation. Nitrogen physisorption reveals a decrease in surface area by nearly a factor of three, to 95 m²/g from 288 m²/g. The measured pore width also decreased to 0.71 nm from 0.88 nm. It is also observed that the material changed color from white to brown after the reactions. It is hypothesized organic species adsorb to the surface and are not removed during the washing and centrifugation steps. The adsorbed species would both decrease the surface area and the catalytic activity. However, the decrease in conversion does not scale proportionally to the decrease in surface area.

TGA/DSC is performed to compare the quantity and identity of adsorbed species on the imogolite catalyst. Figure 6 shows the TGA curves for the as-synthesized IMO and the recycled IMO after three reactions. The mass loss of the recycled IMO is much greater than the as-synthesized material, indicative of more adsorbed species on the material. The initial mass loss of the recycled IMO is lower, which suggests less water adsorbed on the surface. The greater mass

loss of recycled IMO at higher temperatures indicates the presence of organic groups adsorbed on the surface. The results of TGA/DSC corroborate the hypothesis generated from the physical appearance of the material and decrease in surface area

The results of the reuse testing are promising for the use of imogolite in flow reactors as the catalyst does not appear to decompose significantly. Investigation of routes to catalyst regeneration, which would involve desorption of organic species on the surface of the catalyst, would prove useful in making imogolite an effective, reusable catalyst for the continuous conversion of glucose into fructose.

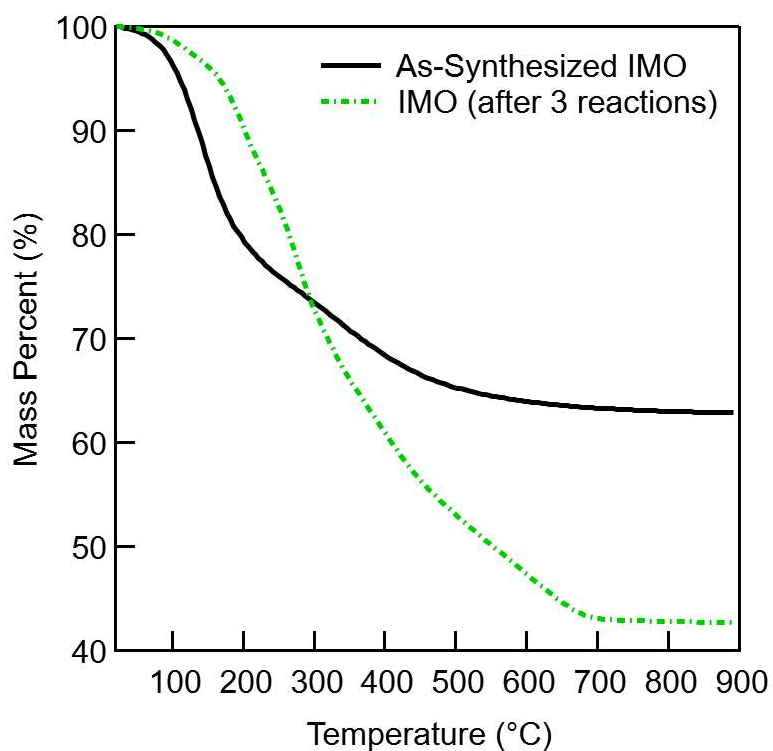


Figure 6: TGA mass loss curve of as-synthesized IMO and recycled IMO after three reactions. The as-synthesized IMO is in black and the recycled IMO is in green.

Chapter 4. Conclusions

The catalytic activity of imogolite nanotubes is investigated for the selective conversion of glucose to fructose. The selectivity for fructose decreases as the conversion of glucose increases. The conversion is shown to increase at elevated reaction temperature. The tunable nature of imogolite demonstrated by introduction of methyl groups and germanium, both achievable through simple changes to the synthesis procedure. These modifications changed the surface properties and catalytic activity of the material. Imogolite nanotubes underwent reuse experiments which showed imogolite undergoes deactivation. The catalyst still maintained selectivity for fructose after recycle. Post-reaction characterization revealed a decrease in surface area and an increase in adsorbed organic species. Overall, the project demonstrates imogolite is an active and tunable catalyst for the isomerization of glucose to fructose.

Bibliography

- [1] L. Shuai, J. Luterbacher, Organic Solvent Effects in Biomass Conversion Reactions, *ChemSusChem*. (2015) n/a-n/a. doi:10.1002/cssc.201501148.
- [2] Y. Román-Leshkov, J.N. Chheda, J.A. Dumesic, Phase modifiers promote efficient production of hydroxymethylfurfural from fructose, *Science* (80-.). 312 (2006) 1933–1937. doi:10.1126/science.1126337.
- [3] S.H. Bhosale, M.B. Rao, V. V Deshpande, Molecular and industrial aspects of glucose isomerase., *Microbiol. Rev.* 60 (1996) 280–300.
<http://mmbbr.asm.org/content/60/2/280.long>.
- [4] M. Moliner, Y. Román-Leshkov, M.E. Davis, Tin-containing zeolites are highly active catalysts for the isomerization of glucose in water., *Proc. Natl. Acad. Sci. U. S. A.* 107 (2010) 6164–6168. doi:10.1073/pnas.1002358107.
- [5] B. Yun Yang, R. Montgomery, Alkaline degradation of glucose: Effect of initial concentration of reactants, *Carbohydr. Res.* 280 (1996) 27–45. doi:10.1016/0008-6215(95)00294-4.
- [6] M. Watanabe, Y. Aizawa, T. Iida, T.M. Aida, C. Levy, K. Sue, H. Inomata, Glucose reactions with acid and base catalysts in hot compressed water at 473 K, *Carbohydr. Res.* 340 (2005) 1925–1930. doi:10.1016/j.carres.2005.06.017.
- [7] V. Choudhary, A.B. Pinar, R.F. Lobo, D.G. Vlachos, S.I. Sandler, Comparison of Homogeneous and Heterogeneous Catalysts for Glucose-to-Fructose Isomerization in Aqueous Media, (2013) 2369–2376. doi:10.1002/cssc.201300328.
- [8] J. Tang, X. Guo, L. Zhu, C. Hu, Mechanistic Study of Glucose-to-Fructose Isomerization in Water Catalyzed by $[\text{Al}(\text{OH})_2/(\text{aq})]^+$, *ACS Catal.* 5 (2015) 5097–5103.
doi:10.1021/acscatal.5b01237.
- [9] C. Liu, J.M. Carraher, J.L. Swedberg, C.R. Herndon, C.N. Fleitman, J.P. Tessonnier, Selective base-catalyzed isomerization of glucose to fructose, *ACS Catal.* 4 (2014) 4295–

4298. doi:10.1021/cs501197w.
- [10] N. Deshpande, L. Pattanaik, M.R. Whitaker, C.T. Yang, L.C. Lin, N.A. Brunelli, Selectively converting glucose to fructose using immobilized tertiary amines, *J. Catal.* 353 (2017) 205–210. doi:10.1016/j.jcat.2017.07.021.
 - [11] N. Rajabbeigi, A.I. Torres, C.M. Lew, B. Elyassi, L. Ren, Z. Wang, H. Je Cho, W. Fan, P. Daoutidis, M. Tsapatsis, On the kinetics of the isomerization of glucose to fructose using Sn-Beta, *Chem. Eng. Sci.* 116 (2014) 235–242. doi:10.1016/j.ces.2014.04.031.
 - [12] C. Moreau, R. Durand, A. Roux, D. Tichit, Isomerization of glucose into fructose in the presence of cation-exchanged zeolites and hydrotalcites, *Appl. Catal. A Gen.* 193 (2000) 257–264. doi:10.1016/S0926-860X(99)00435-4.
 - [13] N. Yoshinaga, S. Aomine, Allophane in some ando soils, *Soil Sci. Plant Nutr.* 8 (1962) 6–13. doi:10.1080/00380768.1962.10430983.
 - [14] V.C. Farmer, A.R. Fraser, J.M. Tait, Synthesis of imogolite: a tubular aluminium silicate polymer, *J. Chem. Soc. Chem. Commun.* (1977) 462. doi:10.1039/c39770000462.
 - [15] S.M. Barrett, P.M. Budd, C. Price, The synthesis and characterization of imogolite, *Eur. Polym. J.* 27 (1991) 609–612. doi:10.1016/0014-3057(91)90144-D.
 - [16] S. Mukherjee, V.M. Bartlow, S. Nair, Phenomenology of the growth of single-walled aluminosilicate and aluminogermanate nanotubes of precise dimensions, *Chem. Mater.* 17 (2005) 4900–4909. doi:10.1021/cm0505852.
 - [17] D.Y. Kang, J. Zang, C.W. Jones, S. Nair, Single-walled aluminosilicate nanotubes with organic-modified interiors, *J. Phys. Chem. C.* 115 (2011) 7676–7685. doi:10.1021/jp2010919.
 - [18] S. Wada, K.O.J. Wada, Effects of Substitution of Germanium for Silicon in Imogolite, *Clays Clay Miner.* 30 (1982) 123–128.
 - [19] A. Thill, P. Maillet, B. Guiose, O. Spalla, L. Belloni, P. Chaurand, M. Auffan, L. Olivi, J. Rose, Physico-chemical control over the single- or double-wall structure of

- aluminogermanate imogolite-like nanotubes, *J. Am. Chem. Soc.* 134 (2012) 3780–3786. doi:10.1021/ja209756j.
- [20] M. Ookawa, M.W.A.J. Anabe, M. Suzuki, Synthesis and Characterization of Fe Containing Imogolite, *Energy*. 284 (2006) 280–284. doi:10.11362/jcssjclayscience1960.12.Supplement2_280.
- [21] Y. Kuroda, K. Fukumoto, K. Kuroda, Uniform and high dispersion of gold nanoparticles on imogolite nanotubes and assembly into morphologically controlled materials, *Appl. Clay Sci.* 55 (2012) 10–17. doi:10.1016/j.clay.2011.07.004.
- [22] G. Ipek Yucelen, R.E. Connell, J.R. Terbush, D.J. Westenberg, F. Dogan, Synthesis and immobilization of silver nanoparticles on aluminosilicate nanotubes and their antibacterial properties, *Appl. Nanosci.* 6 (2015) 607–614. doi:10.1007/s13204-015-0467-x.
- [23] N. Jiravanichanun, K. Yamamoto, K. Kato, J. Kim, S. Horiuchi, W.O. Yah, H. Otsuka, A. Takahara, Preparation and characterization of imogolite/DNA Hybrid Hydrogels, *Biomacromolecules*. 13 (2012) 276–281. doi:10.1021/bm201616m.
- [24] S. Imamura, T. Kokubu, T. Yamashita, Y. Okamoto, K. Kajiwara, H. Kanai, Shape-selective copper-loaded Imogolite catalyst, *J. Catal.* 160 (1996) 137–139. doi:10.1006/jcat.1996.0132.
- [25] S. Imamura, Y. Hayashi, K. Kajiwara, H. Hoshino, C. Kaito, Imogolite: a possible new type of shape-selective catalyst, *Ind. Eng. Chem. Res.* 32 (1993) 600–603. doi:10.1021/ie00016a005.
- [26] S. Konduri, S. Mukherjee, S. Nair, Controlling nanotube dimensions: Correlation between composition, diameter, and internal energy of single- Walled mixed oxide nanotubes, *ACS Nano*. 1 (2007) 393–402. doi:10.1021/nn700104e.
- [27] W.C. Ackerman, D.M. Smith, J.C. Huling, Y.W. Kim, J.K. Bailey, C.J. Brinker, Gas Vapor Adsorption in Imogolite - a Microporous Tubular Aluminosilicate, *Langmuir*. 9 (1993) 1051–1057.

- [28] J.M. de Bruijn, A.P.G. Kieboom, H. van Bekkum, Alkaline degradation of monosaccharides V: Kinetics of the alkaline isomerization and degradation of monosaccharides, *Recl. Des Trav. Chim. Des Pays-Bas.* 106 (1987) 35–43. doi:10.1002/recl.19871060201.
- [29] J.M. De Bruijn, A.P.G. Kieboom, H. van Bekkum, Alkaline Degradation of Monosaccharides Part VII. A Mechanistic Picture, *Starch - Stärke.* 39 (1987) 23–28. doi:10.1002/star.19870390107.
- [30] P.D.G. Cradwick, V.C. Farmer, J.D. Russell, C.R. Masson, K. Wada, N. Yoshinaga, Imogolite, a Hydrated Aluminium Silicate of Tubular Structure, *Nat. Phys. Sci.* 240 (1972) 187–189. doi:10.1038/phyci240187a0.
- [31] X. Yang, Z. Sun, D. Wang, W. Forsling, Surface acid-base properties and hydration/dehydration mechanisms of aluminum (hydr)oxides, *J. Colloid Interface Sci.* 308 (2007) 395–404. doi:10.1016/j.jcis.2006.12.023.

Appendix A. Supplementary Information

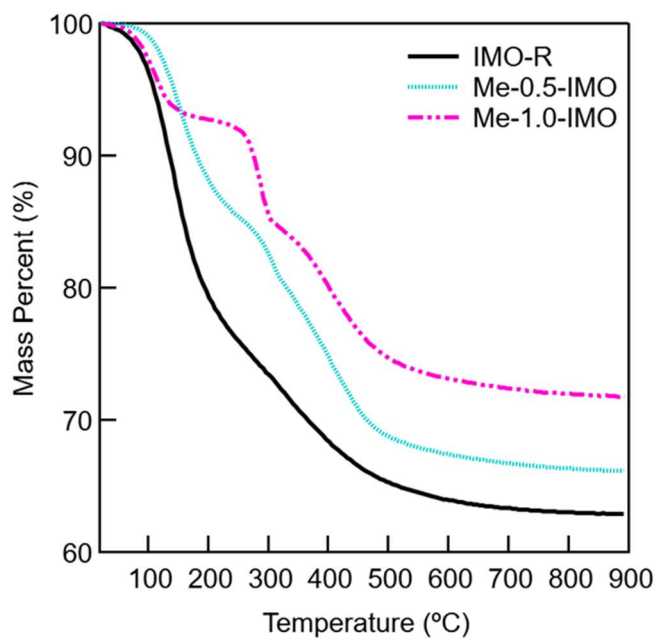


Figure S1: TGA mass loss curves for AlSi IMO and IMO modified with 50 and 100% methyl.

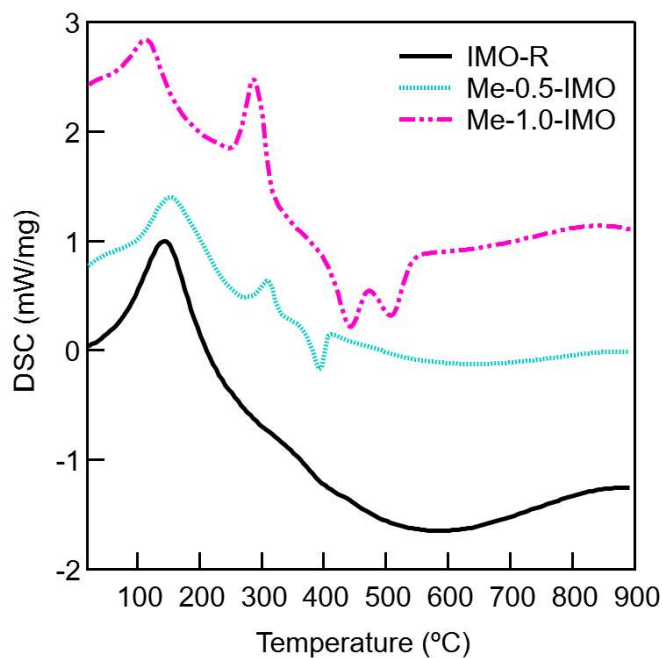


Figure S2: DSC curves for AlSi IMO and IMO modified with 50 and 100% methyl. Downward pointing peaks indicate exothermic reactions.

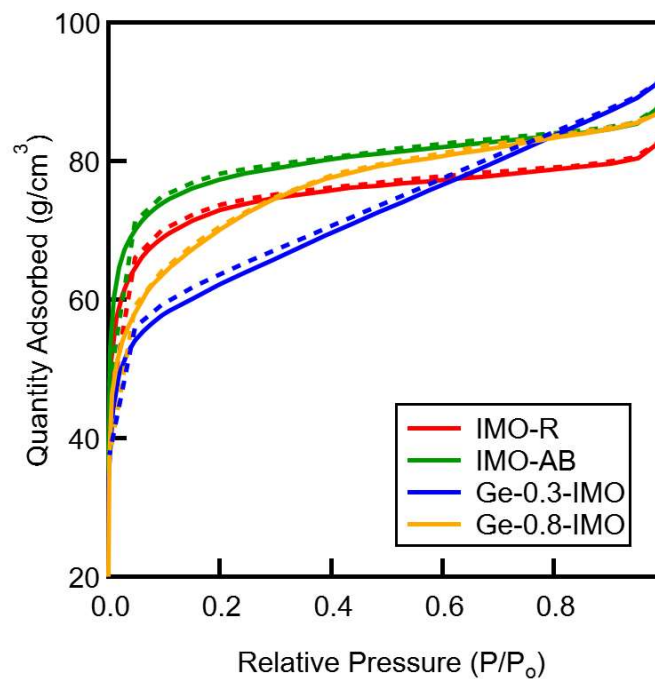


Figure S3: Nitrogen physisorption isotherms for IMO-R and IMO-AB compared to IMO of 30% and 80% Ge.

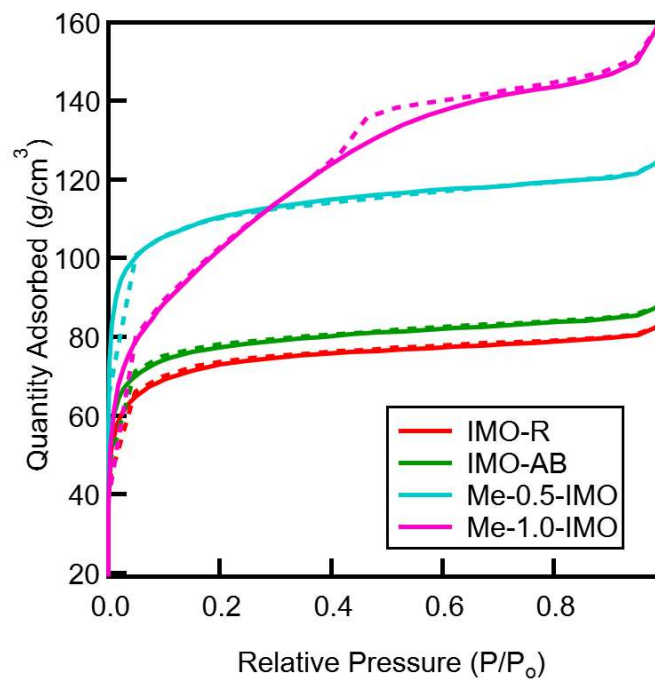


Figure S4: Nitrogen physisorption isotherms for IMO-R and IMO-AB compared to IMO of 50% and 100% methyl.

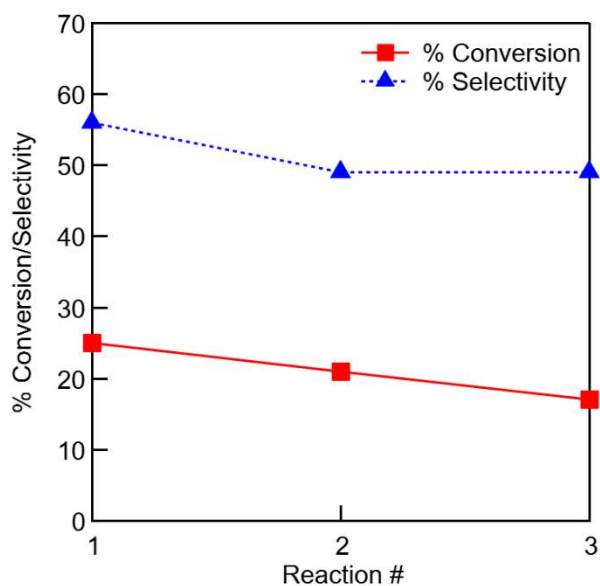


Figure S5: Change in conversion and selectivity for the recycle tests of IMO.

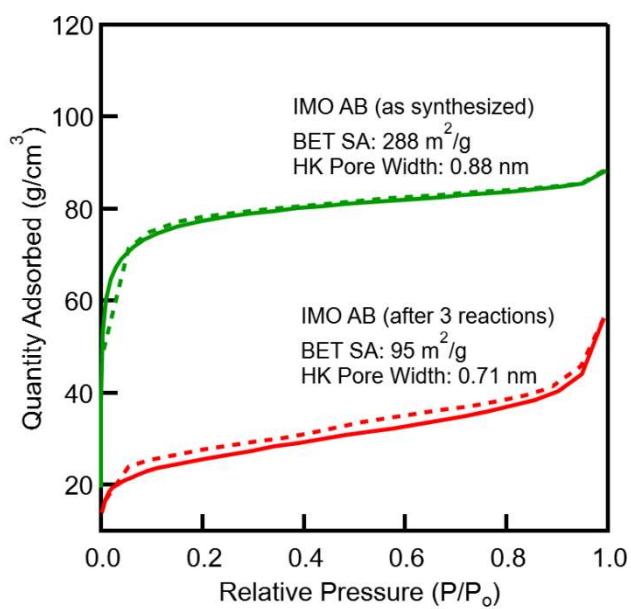


Figure S6: Nitrogen physisorption isotherms of IMO as-synthesized and IMO after three reactions. The su